Received: 5 May 2021 | Revised: 10 August 2021 | Accepted: 16 August 2021

DOI: 10.1002/app.51606

ARTICLE

Applied Polymer SCIENCE WILEY

Acid catalyzed cross-linking of polyvinyl alcohol for humidifier membranes

Andre Michele[1] | **Patrick Paschkowski**[2] | **Christopher Hänel**[2] | **Günter E. M. Tovar**[1] | **Thomas Schiestel**[2] | **Alexander Southan**[1]

[1]Institute of Interfacial Process Engineering and Plasma Technology IGVP, University of Stuttgart, Stuttgart, Germany

[2]Innovation Field Membranes, Fraunhofer Institute for Interfacial Engineering and Biotechnology IGB, Stuttgart, Germany

Correspondence
Alexander Southan, Institute of Interfacial Process Engineering and Plasma Technology IGVP, University of Stuttgart, Nobelstr. 12, 70569 Stuttgart, Germany.
Email: alexander.southan@igvp.uni-stuttgart.de

Funding information
Bundesministerium für Wirtschaft und Energie, Grant/Award Number: 03ET6091D

Abstract

Polyvinyl alcohol (PVA) is a hydrophilic polymer well known for good film forming properties, high water vapor permeance J_W, and low nitrogen permeance. However, depending on molar mass and temperature, PVA swells strongly in water until complete dissolution. This behavior affects the usability of PVA in aqueous environments and makes cross-linking necessary if higher structural integrity is envisaged. In this work, PVA networks are formed by thermal cross-linking in the presence of *p*-toluenesulfonic acid (TSA) and investigated in a design of experiments approach. Experimental parameters are the cross-linking period t_c, temperature ϑ and the TSA mass fraction w_{TSA}. Cross-linking is found to proceed via ether bond formation at all reaction conditions. Degradation is promoted especially by a combination of high w_{TSA}, t_c and ϑ. Thermal stability of the networks after preparation is strongly improved by neutralizing residual TSA. Humidification membranes with a J_W of 6423 ± 63.0 gas permeation units (GPU) are fabricated by coating PVA on polyvinyliden fluoride hollow fibers and cross-linking with TSA. Summarizing, the present study contributes to a clearer insight into the cross-linking of PVA in presence of TSA, the thermal stability of the resulting networks and the applicability as selective membrane layers for water vapor transfer.

KEYWORDS

coatings, cross-linking, gels, membranes, swelling

1 | INTRODUCTION

Polyvinyl alcohol (PVA) is a widely used polymer for many applications, for example, humidity sensors,[1] adsorption of dyes,[2] hydrogel scaffolds for tissue engineering,[3] drug delivery systems,[4] and semipermeable membranes for filtration in water treatment[5–7] or the humidification of air.[8,9] It is a hydrophilic polymer that shows good anti fouling properties,[10] film forming properties which allow the deposition of thin films,[11] temperature stability up to 250°C[12] and good water vapor selectivity against nitrogen.[13] Moreover, PVA swells in water until it dissolves completely. To overcome this disadvantage, cross-linking of PVA is necessary before it can be used in aqueous environments. Cross-linking decreases the equilibrium degree of

This is an open access article under the terms of the Creative Commons Attribution License, which permits use, distribution and reproduction in any medium, provided the original work is properly cited.
© 2021 The Authors. *Journal of Applied Polymer Science* published by Wiley Periodicals LLC.

swelling (*EDS*) and prevents complete dissolution of the polymer.[14]

Numerous cross-linking methods for PVA are described in the literature. They can be divided into two categories, physical cross-linking and chemical cross-linking. Physical cross-linking is based on, for example, molecular entanglements, physical interactions like hydrogen bonds, or ordered crystalline areas. Physical PVA networks can be prepared, for example, via a freeze–thaw method[15] or heat treatment.[16,17] However, crystallinity is undesirable for membrane applications as it lowers the free volume necessary for the diffusion of permeants.[15,18]

Chemically cross-linked PVA is linked together via covalent bonds. Therefore, no crystallinity is needed to reach insolubility. The most prominent chemical cross-linker for PVA is the bifunctional glutaraldehyde. Disadvantages of this method are the two-step process, the need for corrosive hydrochloric acid as catalyst, high immersion times to reach low degrees of swelling, and the toxicity and carcinogenicity of glutaraldehyde.[9,14,19,20]

Another possibility of chemically cross-linking PVA is thermal treatment in the presence of acids, for example, sulfuric acid, hydrochloric acid, and sulfonic acids. Immelman et al.[21] stated that thermal treatment of PVA at 100 to 125°C in the presence of sulfuric acid induces ether-bond formation between the PVA chains. Simultaneously, hydroxyl groups of the PVA were eliminated and conjugated double bonds were formed in the chain, which made the polymer turn black. The mechanisms of these reactions are stated to be similar to those of low molecular alcohols. Hence, a higher temperature favors the elimination (E_1) over ether-bond formation via nucleophilic substitution.[22] However, an insolubilization of PVA in water may be achieved by both reactions. Drechsel and Görlich[23] showed that the presence of strong acids like sulfuric acid and hydrochloric acid enabled dehydration of PVA at 80, 100, and 120°C. Since the hydrophilicity of PVA is crucial for many applications, unintended elimination of hydroxyl groups is disadvantageous and should be avoided while cross-linking. Xu et al.[24] esterified PVA with sulfuric acid. The sulfated PVA (sPVA) was thermally cross-linked at 120°C for 3 h. They stated that this occurs due to the self-cross-linking between the monoester of the sulfuric acid and the hydroxyl groups of PVA. The thermal stability of membranes decreased with increasing sPVA content. Choudhury et al.[25] synthesized the statistical copolymer poly(vinyl alcohol-*co*-styrenesulfonic acid) via free radical polymerization. They stated, that the polymer could be used for water purification or fuel cell membranes because of its good cross-linking ability, film forming characteristics, hydrophilicity, water-retaining capacity at higher temperature, and proton conducting sites. However, changing the acid from sulfuric acid to a sulfonic acid adds the option of sulfonic ester bonds, which are more labile to hydrolysis in presence of water than ether bonds.[26,27] Saito[28] et al. casted a solution of PVA and poly(styrenesulfonic acid) (PSSA) on a flat poly(methyl methacrylate) plate and dried it at 25°C for 7 days. These membranes were annealed at 140 or 180°C under vacuum for 40 min to decrease the degree of hydration. Koyama et al.[29] prepared reverse osmosis membranes by casting a solution of PVA and PSSA and heat cured at 120°C for 2 h. They stated that the membrane was cross-linked by the formation of R—O—SO_2—R bonds and intermolecular dehydration of PVA. These bonds were not formed in presence of the sodium salt of PSSA (NaPSSA) which stresses the important role of the acidic proton for cross-linking PVA in presence of a sulfonic acid with heat. It was not stated to which degree the insolubility of the network relates to intermolecular dehydration of PVA or the formation of cross-links between PVA and PSSA.

Since the stability of the networks against hydrolysis in water relates to the kind of bonds formed between the PVA polymer chains, a study on the cross-linking mechanism should be executed. Moreover, it is crucial to monitor the cross-linking progress depending on the cross-linking parameters to receive a PVA network with the desired insolubility and swelling properties in water, whilst minimizing the progress of side reactions and process duration. We hypothesize that *p*-toluenesulfonic acid (TSA), a low molecular weight compound, may be capable of cross-linking polyvinyl alcohol (PVA) by catalyzing the intermolecular condensation reaction of the alcoholic hydroxyl groups via the acidic proton, analogous to sulfuric acid and other sulfonic acids, for example, PSSA. TSA has not been used for this purpose so far. An advantage of TSA compared to sulfuric acid could be its higher pK_a value (−8.3 compared to −6.57),[30,31] thus mitigating side reactions, especially elimination reactions. Additionally, TSA is less volatile and corrosive than sulfuric acid, making its use in fabrication processes more likely.[32] TSA cannot entangle into the cross-linked PVA network like PSSA. Therefore, it might be possible to neutralize the TSA after cross-linking, which makes it suitable for investigations of the cross-linking progress and the thermal stability of PVA networks cross-linked in presence of a sulfonic acid.

Therefore, in this contribution PVA was heat-treated in presence of TSA to obtain insoluble polymer networks. The influence of the temperature (ϑ), treatment period (t_c) and TSA mass fraction (w_{TSA}) on cross-linking were monitored in a design of experiments approach by measuring the gel content (Y) and equilibrium degree of

swelling (*EDS*). Furthermore, it was attempted to clarify the chemical reaction responsible for cross-linking. The thermal stability of the received PVA networks was examined via thermogravimetric analysis (TGA), Fourier transform infrared (FT-IR) spectroscopy, as well as the heat treatment gel content Y_h and *EDS* at 120°C in dry and excess humidified air for 7 days. The applicability of the cross-linked PVA as a selective layer in a composite humidification membrane was demonstrated by dip coating thin PVA films on polyvinyliden fluoride (PVDF) hollow fibers. The films were heat cross-linked in presence of TSA to create stable membranes with good water vapor permeance and high selectivity against nitrogen.

2 | EXPERIMENTAL SECTION

2.1 | Materials

Polyvinyl alcohol (PVA, Mowiol 6–98, M_w 47,000, 98% hydrolyzed), *p*-toluenesulfonic acid monohydrate (TSA, 98%), sodium hydroxide (NaOH, 98%), and chloroform-d ($CDCl_3$, 99.8%) were purchased from Sigma-Aldrich. Silica gel 60 (0.06–0.2 mm) and *N*-ethyl-2-pyrrolidone (NEP, 99.8%) were purchased from Carl Roth and 2-propanol (99%) from Fisher Scientific. Polyvinylidenfluoride (PVDF, KF1550) was kindly provided from Kureha and polyvinylpyrrolidone (PVP, Kollidon KF17PF) from BASF. The above-mentioned materials were used as received. Argon N50 was purchased from Air Liquide and dried by passing through an Agilent "Gas Clean Moisture" filter prior to use.

2.2 | Preparation of cross-linked polyvinyl alcohol networks

PVA networks were prepared by a solvent casting method. For this purpose, hydrogel precursor solutions with a PVA concentration of $c_{PVA} = 176\ g\ L^{-1}$ and a TSA mass fraction of $w_{TSA} = 5\%$, 10%, and 15% relative to the PVA mass were prepared in water as follows: 3.529 g PVA were dissolved in 17 ml demineralized water (electrical conductivity $G = 0.055\ \mu S\ cm^{-1}$) at 80°C. 0.176 g (0.012 eq., $w_{TSA} = 5\%$), 0.353 g (0.023 eq., $w_{TSA} = 10\%$) or 0.529 g (0.035 eq., $w_{TSA} = 15\%$) TSA were dissolved in 3 ml demineralized water, respectively. Each TSA solution was added to a separate PVA solution and stirred for 30 min while letting the mixture cool down to room temperature. The solutions were poured into polystyrene petri dishes and dried for 12 h at 40°C and ambient pressure in a furnace (VDL 53 or ED 240, Binder), followed by 12 h at 40°C under reduced pressure (40 mbar) in a vacuum furnace (VDL 115, Binder). Transparent specimens composed of PVA with TSA mass fractions w_{TSA} of 5%, 10%, and 15% were formed. These specimens were weighed for their initial mass m_0 and cross-linked at various temperatures ϑ for various periods t_c in the above-mentioned furnaces. ϑ and t_c were set to 120, 140, and 160°C as well as 60, 75, and 90 min, respectively. The cross-linked PVA networks were washed with aqueous NaOH solution (0.05 mol L^{-1}) for 3 h at 90°C followed by washing with water for 12 h at 90°C. The so formed hydrogels were weighed for their swollen mass m_w, at room temperature, dried for 12 h at 40°C under reduced pressure (40 mbar) and weighed again for their dry mass m_d.

Samples will be named by their preparation parameters as follows: a PVA network cross-linked with $w_{TSA} = 5\%$ at 120°C for 60 min which was washed with sodium hydroxide solution and water and dried afterwards, will be referred to as PT-5-120-60-s. The same network which was washed with water only will be named PT-5-120-60-w and without any washing step PT-5-120-60. Gel contents Y and equilibrium degrees of swelling *EDS* were calculated as follows:

$$Y = \frac{m_d}{m_0}, \tag{1a}$$

$$EDS = \frac{m_w}{m_d}. \tag{1b}$$

2.3 | Design of experiments and statistics

We followed a two-level full factorial design (2^3) with an added center point to investigate the cross-linking reaction of PVA in the presence of TSA. Thus, the experimental design has two levels for each of the three parameters ϑ, t_c and w_{TSA}, which are equal to the border values of the parameter space. The tested parameter values are shown in Table 1 together with their transformation to coded parameter values (see Table S1 in the supporting information for a list of all parameter combinations tested). The dimensionless coded values were obtained by setting the lower parameter values to −1, the center point

TABLE 1 Conversion table of coded parameter values (-1, 0, 1) used for data analysis to actual parameter values used for investigation of polyvinyl alcohol cross-linking with *p*-toluenesulfonic acid

Coded values	-1	0	1
t_c	60 min	75 min	90 min
w_{TSA}	5%	10%	15%
ϑ	120°C	140°C	160°C

to 0 and the higher parameter values to 1. All experiments with parameter combinations with high and low parameter values were performed in triplicates, the center point was measured 12 times.

Data were analyzed with the software DesignExpert 12 (Stat-Ease). A full linear model was used to describe the experimentally determined responses R:

$$R = r_0 + a_\vartheta \cdot \vartheta + a_t \cdot t_c + a_{\mathrm{TSA}} \cdot w_{\mathrm{TSA}} + b_{\vartheta,\mathrm{t}} \cdot \vartheta \cdot t_\mathrm{c} + b_{\vartheta,\mathrm{TSA}} \cdot \vartheta \cdot w_{\mathrm{TSA}} + b_{\mathrm{t,TSA}} \cdot t_\mathrm{c} \cdot w_{\mathrm{TSA}} + c_{\vartheta,\mathrm{t,TSA}} \cdot \vartheta \cdot t_\mathrm{c} \cdot w_{\mathrm{TSA}}. \tag{2}$$

Here, a_ϑ, a_t, a_{TSA}, $b_{\vartheta,\mathrm{t}}$, $b_{\vartheta,\mathrm{TSA}}$, $b_{t,\mathrm{TSA}}$ and $c_{\vartheta,\mathrm{t,TSA}}$ are regression coefficients, the regression was performed both with coded as well as actual parameter values. Statistical significance of the model terms was determined by analysis of variance (ANOVA), and non-significant model terms with p-values greater than 0.05 were excluded. Analyzed responses were Y and EDS. For the EDS, the data was transformed with an inverse square root $EDS' = (\sqrt{EDS})^{-1}$ to compensate the curvature.

All errors shown are SDs of the measured values, including the thermal stability experiments, water transfer measurements and nitrogen permeances. The errors of the selectivities of the membranes ΔQ_{WN} were calculated via propagation of uncertainity (Equation S1 in supporting information).

2.4 | Measurement of the decomposition temperatures of polyvinyl alcohol networks

PVA networks were prepared as described above with ϑ at 120°C and a t_c of 60 min. Then thermogravimetric analysis was performed with an "STA 449 F3 Jupiter" (Netzsch, Germany) in ceramic Al_2O_3 pans. For TGA, samples were cut into pieces and 20 ± 2 mg of those were weighed into ceramic Al_2O_3 pans without lid. The TGA scans were executed with a heating rate of 10 K min^{-1} in the range of 35–600°C under synthetic air (80% N_2, 20% O_2). Crude PVA "Mowiol 6-98" was measured in the same conditions. The temperature of the onset of the mass loss was determined via the software "Origin" (Version 2019b; OriginLab Corporation; Northampton, USA) and used as decomposition temperature ϑ_d.

2.5 | Thermal stability test for polyvinyl alcohol networks

PVA networks were prepared according to the procedure above with ϑ at 120°C and a t_c of 60 min and weighed for their dry mass m_d. The samples were divided in half and one-half was placed in a furnace (VDL 53, Binder). To observe the influence of relative humidity on the thermal stability, the other half was placed in a pressure cooker (P2530738 Secure 5 Neo V2, Tefal, France) which was partly filled with water. The specimens were not in direct contact with the liquid water. The treatment in dry and wet atmosphere was performed at 120°C with heat treatment periods t_h of 3, 12, 24, 48, and 168 h, respectively. For each t_h a separate network was fabricated. After the treatment, unbound polymer was removed from the PVA networks by extraction with water at 90°C for 12 h and the samples were dried for 12 h at 40°C under reduced pressure (40 mbar). Then the networks were weighed again for their dry mass m_{d2}. The ratio of the gel content after the stability test Y_2 and Y was calculated resulting in the heat treatment gel content Y_h.

$$Y_2 = \frac{m_{\mathrm{d2}}}{m_0}, \tag{3}$$

$$Y_\mathrm{h} = \frac{Y_2}{Y} = \frac{m_{\mathrm{d2}}}{m_\mathrm{d}}. \tag{4}$$

EDS, as well as attenuated total reflection Fourier transform infrared (ATR FT-IR) spectra of the networks were measured before and after heat treatment. The FT-IR spectra were recorded on a "Vertex70" spectrometer (Bruker) using a diamond ATR crystal. The FT-IR measurements were executed in the range of 4000–500 cm^{-1}. The baseline of the spectra was corrected with the software OPUS (Bruker). The spectra were then normalized to the CH-stretch vibration at 2900–3000 cm^{-1} in order to account for the different amount of absorbing molecules.

2.6 | Model reaction of 2-propanol with *p*-toluenesulfonic acid

As a model compound for PVA, 2-propanol was used to investigate the chemical reactions of a secondary alcohol in the presence of TSA. 2-propanol was reacted with TSA for different reaction periods with varying stoichiometric ratios of 2-propanol, TSA and silica gel (as a drying agent to remove water formed by the reaction) in a pressure reactor (tinyclave steel, Büchi). As an example, a reaction of a tenfold molar excess of 2-propanol relative to TSA is described, all other reactions were performed similarly with different amounts. 1.24 g (6.5 mmol, 0.1 eq) *p*-toluenesulfonic acid was dissolved in 3.9 g 2-propanol (65 mmol, 5 ml, 1.0 eq) in a pressure reactor, and 0.26 g

silica gel 60 (pore diameter 0.06–0.2 mm) were added while stirring the solution. The reactor was flushed with Argon, sealed and then heated with an oil bath until the overpressure in the reactor reached 2.5 bar, which is approximately the vapor pressure of 2-propanol at 120°C.[33,34] 2.5 bar overpressure were reached with an oil bath temperature of 140°C. The temperature was kept constant for 1 h (reaction period). To terminate the reaction, the pressure reactor was cooled down to room temperature with a water bath and opened. The solution was filtered to separate the silica gel and the filtrate was analyzed via ^{1}H-NMR spectroscopy (Avance 500, Bruker) without further purification (spectra in Figure S1, supporting information).

^{1}H NMR ($C\mathbf{D}Cl_3$, 500 MHz, δ): 1.10 (d, $J = 6.1$ Hz, 12 H, $(C\mathbf{H}_3)_2$-CH-O-CH-$(C\mathbf{H}_3)_2$), 1.16 (d, $J = 6.2$ Hz, 6 H, HO-CH-$(C\mathbf{H}_3)_2$), 2.32 (s, 3 H, Ar-$C\mathbf{H}_3$), 3.62 (st, $J = 12.2$ Hz, 2 H, **H**C-O-C**H**), 4.0 (st, $J = 12.3$ Hz, 1 H, HO-C**H**), 5.54 (s, 1 H, $SO_3\mathbf{H}/H_3O^+$), 7.15 (d, $J = 8.0$ Hz, 2 H, Ar-**H** meta to SO_3H), 7.26 (s, $C\mathbf{D}Cl_3/C\mathbf{H}Cl_3$) 7.69 (d, $J = 8.2$ Hz, 2 H, Ar-**H** ortho to SO_3H).

The molar fraction χ and the amount n_{ether} of diisopropyl ether relative to the starting amount n_{TSA} of TSA using the starting amount n_0 of 2-propanol were calculated with Equations 5a and 5b, respectively (for results see Table S2 in the supporting information).

$$\chi = \frac{\frac{1}{2}\int \text{diisopropylether } \mathbf{H}C-O-C\mathbf{H}}{\int \text{isopropanol } HO-C\mathbf{H} + \frac{1}{2}\int \text{diisopropylether } \mathbf{H}C-O-C\mathbf{H}}, \tag{5a}$$

$$\frac{n_{\text{Ether}}}{n_{\text{TSA}}} = \frac{\chi}{\chi+1} \cdot \frac{n_0}{n_{\text{TSA}}}. \tag{5b}$$

The ratio specified by Equation 5b can be understood as average number of reactions one molecule of TSA is participating in.

2.7 | Fabrication and coating of membranes

PVDF hollow fibers were fabricated through nonsolvent-induced phase separation (NIPS) and coated via a continuous dip coating process. The procedure was described in detail in a previous work.[9] In short, 45 g PVDF and 45 g PVP were dissolved in 210 g of NEP. The solution was spun through a spinneret (Central fluid: 75% NEP/25% DI-water v/v) with an outer diameter $d_o = 1.0$ mm and an inner diameter $d_i = 0.5$ mm into a coagulation bath (DI-water). The resulting hollow fiber (HF) membranes ($d_o = 2.0$ mm, $d_i = 1.57$ mm) had a nitrogen permeance of more than 100 m^3 m^{-2} h^{-1} bar^{-1}. To reduce the nitrogen permeance, the HF were coated with an aqueous solution of $w_{\text{PVA}} = 5\%$ and $w_{\text{TSA}} = 10\%$ relative to the PVA. A dip-coating process was used in a roll-to-roll device with a coating velocity of 1 m min^{-1}.[9] The thin PVA layers were cross-linked via heat treatment at $\vartheta = 120$°C with t_c of 60, 75, 90 , 120, and 180 min. The fibers were washed as described for the PVA networks above.

2.8 | Determination of the water vapor and nitrogen permeance

Pure nitrogen permeance J_N was measured as a mean value for the gas leakage before and after the water transfer measurement (WTR-M). An "ADM" flowmeter (Agilent Technologies) was used which measures gas flows volumetrically. All flowmeters and mass flow controllers were calibrated for normal temperature and pressure (NTP, 273.15 K and 1 atm) to respect the dependence of the gas volume on the measurement conditions. In this work, NTP is indicated by a subscript "n" in the symbol and unit, that is, the normal airflow $\dot{V}_n$ and the normal nitrogen flow $\dot{V}_{nN}$, both with the unit L_n h^{-1}.

For the measurement of J_N, nitrogen was applied at 0.5, 1, 1.5, and 2 bar inside the hollow fiber and the gas flow on the outside was measured using the flowmeter. Dividing the resulting $\dot{V}_{nN}$ through the membrane surface area A and the applied pressure values Δp yields J_N:[9]

$$J_N = \frac{\dot{V}_{nN}}{A \cdot \Delta p}. \tag{6}$$

A two factorial ANOVA with Bonferroni correction (significance level $\alpha = 0.05$) was applied to assess if t_c and the WTR-M had a significant influence on J_N. The water vapor flux was determined with a setup already described in a previous work.[9] Two airflows are passed in counterflow over the membrane. While the airflow through the hollow fiber inside is dry, the flow on the outside of the membrane previously passes through a washing flask with water to humidify the gas. Two sensors measure temperature and relative humidity RH, one for the humid air influent flow, later referred to as "wet in". The other sensor measured the outlet flow of the dry side, so-called "dry out". The whole setup is built into a cabinet, so the measurement can be undertaken at different measurement temperatures ϑ_P. In this work, ϑ_P was adjusted between 60 and 90°C. $\dot{V}_n$ was set between 20 and 200 mL_n min^{-1} on both sides of the membrane using mass flow controllers (Bronkhorst). The mass related water vapor flow rate $\dot{m}_w$ was then calculated

with the relative humidity of the dry out stream. Dividing $\dot{m}_w$ by the membrane area A yields the water transfer rate WTR:

$$\mathrm{WTR} = \frac{\dot{m}_w}{A}. \tag{7}$$

The water vapor permeance J_w was calculated assuming an ideal gas behavior via the following equation:[9,35]

$$J_w = \frac{\dot{V}_{nw}}{A \cdot \left(p_{feed} - p_{perm}\right)}. \tag{8}$$

Here, p_{feed} is the water vapor partial pressure on the feed side and p_{perm} on the permeate side, and $\dot{V}_{nN}$ the volume related water vapor flow rate. The transformation of Equation 8 to calculate J_W with the WTR and the derivation of unit converting factors for J_W and J_N to gas permeation units (GPU) are given in section 5 in the supporting information. The ratio of water vapor permeance against nitrogen permeance Q_{WN} was calculated with Equation 9.

$$Q_{WN} = \frac{J_W}{J_N} \tag{9}$$

J_N was always calculated using the value measured at $\vartheta_P = 25°C$ with dry nitrogen, while J_w was calculated using $\dot{m}_w$ values determined at ϑ_P between 60 and 90°C with humidified air.

3 | RESULTS AND DISCUSSION

3.1 | Cross-linking of polyvinyl alcohol in presence of *p*-toluenesulfonic acid

The aim of the cross-linking process is the preparation of an insoluble network of covalently cross-linked PVA chains, which is still hydrophilic and able to swell in water, resulting in hydrogels. A good way of measuring the percentage of cross-linked material is the determination of the gel content Y (Equation 1a), which corresponds to the fraction of starting polymer that became insoluble during treatment. The hydrophilicity and free volume is correlated to the equilibrium degree of swelling EDS, which corresponds to the amount of water a hydrogel can absorb (Equation 1b). To optimize Y and EDS, the best operation point for cross-linking was examined by a design of experiment approach varying the cross-linking temperature ϑ, cross-linking period t_c and TSA weight fraction w_{TSA}.

In order to define the parameter borders for the experimental design, preliminary experiments showed that at ϑ of 100°C, no insoluble material was formed at w_{TSA} between 5% and 15% by applying t_c up to 120 min. Furthermore no intact hydrogels were received from experiments made with cross-linking periods below 60 min. Insoluble PVA networks were obtained at all combinations of ϑ values of 120 and 160°C, t_c values of 60 and 90 min and w_{TSA} values of 5% and 15%. Therefore, these parameter values were used as borders for the parameter space covered by the model resulting from the experimental design. The experimentally determined values for Y and EDS are shown in Figures 1 and 2, respectively.

In the first step, the experimental data were analyzed for statistically significant effects by analysis of variance. Both resulting models (Y and EDS') are significant in terms of statistical measures with p-values $<10^{-4}$. The p-values for all cross-linking and interaction parameters are listed in Table 2. In the model for Y, all interaction terms were significant as well as the cross-linking parameters ϑ and t_c. The p-value for w_{TSA} was 0.445 and w_{TSA} can therefore be considered to not have a significant effect on Y. However, w_{TSA} was included into the model in order to maintain hierarchy. In the EDS' model, all cross-linking parameters were significant as well as the interaction terms $\vartheta \cdot t_c$ and $\vartheta \cdot w_{TSA}$. The interaction term $t_c \cdot w_{TSA}$ and the three factor interaction term were excluded from the model due to p-values >>0.05. The $\vartheta \cdot w_{TSA}$ term has a p-value of 0.0775 and is therefore exceeding the 0.05 significance level threshold. The

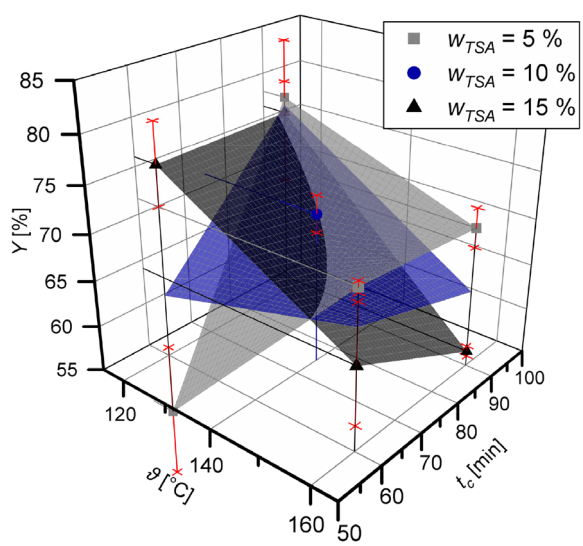

FIGURE 1 Gel contents Y of polyvinyl alcohol cross-linked according to the experimental design explained in the text. The measured Y values were fitted to a linear model given by Equation 2, taking only the statistically significant parameters into account [Color figure can be viewed at wileyonlinelibrary.com]

parameter was nonetheless incorporated into the model, as the *p*-value was only slightly higher than the threshold value and the effect on the *EDS′* was reasonably high. The lack of fit for the *EDS′* model was not significant with a *p*-value of 0.252, whereas for *Y* there was no degree of freedom left to check the significance of the lack of fit.

The statistical evaluation of the cross-linking reaction of PVA with TSA showed that the experimental outcome is influenced by a variety of parameters and parameter interactions, making data interpretation rather complex. In order to understand the effects of different parameter combinations in detail, the experimental data were fitted with the model described by Equation 2 using coded parameter values and only the statistically significant model terms. The resulting values of the regression coefficients are shown in Table 3. The value of r_0 describes the value of the model center point (coded parameter values all zero). Using the coded parameter values has the advantage that the absolute values of the regression coefficients can be used directly to compare the influence of the different parameters on the response value.

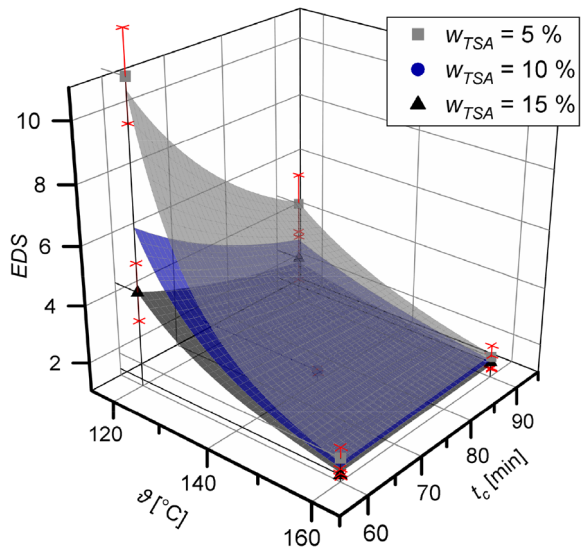

FIGURE 2 Equilibrium degrees of swelling *EDS* of polyvinyl alcohol cross-linked according the experimental design explained in the text. The measured *EDS′* were fitted to a linear model given by Equation 2, taking only the statistically significant parameters into account. For the sake of a more intuitive understanding, *EDS′* was transformed back to *EDS* for the figure [Color figure can be viewed at wileyonlinelibrary.com]

First looking at *Y*, this meant that the highest value was predicted at the combination of a low ϑ ($a_\vartheta < 0$), a high t_c ($a_t > 0$), and a low w_{TSA} (although $a_{TSA} > 0$). With this parameter value combination, also the interaction terms $\vartheta \cdot t_c$, $t_c \cdot w_{TSA}$ and $\vartheta \cdot t_c \cdot w_{TSA}$ resulted in an increase of *Y* ($b_{\vartheta,t} < 0$, $b_{t,TSA} < 0$ and $c_{\vartheta,t,TSA} > 0$) that outweighed the decrease caused by the negative contribution of $\vartheta \cdot w_{TSA}$ ($b_{\vartheta,TSA} < 0$). In fact, with 76%, the highest values for *Y* were found at $\vartheta = 120°C$ (low) and $t_c = 90$ min (high) with only a minor influence of w_{TSA} (Figure 1). A similar reasoning explained the lowest *Y* of 48% ± 8.0% at $\vartheta = 120°C$ (low), $t_c = 90$ min (low) and $w_{TSA} = 5\%$ (low). For a better overview, all possible combinations of high/low parameter values together with their effect on *Y* are shown in Table S3 (Supporting Information).The parameter interactions resulted in an increase of *Y* at a low w_{TSA} with ϑ and t_c from 48% ± 8.0% at 120°C and 60 min to 70% ± 2.0% at 160°C and 90 min. At w_{TSA} of 15%, this trend turned vice versa. With t_c of 90 min, *Y* decreased from 76% ± 8.0% to 64% ± 6.0% by raising ϑ from 120 to 160°C.

TABLE 2 *p*-values for the cross-linking parameters temperature ϑ, period t_c and weight fraction w_{TSA} of *p*-toluenesulfonic acid, as well as *p*-values for the two factor interaction parameters $\vartheta \cdot t_c$, ϑw_{TSA}, $t_c \cdot w_{TSA}$ and the three factor interaction parameter $\vartheta \cdot t_c \cdot w_{TSA}$. The interaction parameters $t_c \cdot w_{TSA}$ and $\vartheta \cdot t_c \cdot w_{TSA}$ were excluded in the *EDS* model due to *p*-values >0.05. The cross-linking parameter w_{TSA} was included into the *Y* model despite its high *p*-value in order to maintain a hierarchical model

	Model	ϑ	t_c	w_{TSA}	$\vartheta \cdot t_c$	$\vartheta \cdot w_{TSA}$	$t_c \cdot w_{TSA}$	$\vartheta \cdot t_c \cdot w_{TSA}$
Y	$<10^{-4}$	2.21×10^{-2}	2.30×10^{-3}	4.45×10^{-1}	$<10^{-4}$	$<10^{-4}$	$<10^{-4}$	1.10×10^{-4}
EDS′	$<10^{-4}$	$<10^{-4}$	1.17×10^{-2}	$<10^{-4}$	2×10^{-4}	7.75×10^{-2}	–	–

TABLE 3 Regression coefficients from Equation 2 using coded parameter values and only including significant model terms from Table 2. The values obtained using the coded parameter values allow to compare the effects of the different model terms on *Y* and *EDS'*, respectively

	r_0	a_ϑ	a_t	a_{TSA}	$b_{\vartheta,t}$	$b_{\vartheta,TSA}$	$b_{t,TSA}$	$c_{\vartheta,t,TSA}$
Y	67.6	−1.96	2.71	6.5×10^{-1}	−4.87	−5.96	−4.46	2.96
EDS′	64.1×10^{-2}	16.8×10^{-2}	3.06×10^{-2}	6.82×10^{-2}	-4.82×10^{-2}	-2.08×10^{-2}	–	–

Interestingly, the model for *EDS′* did not reflect the full complexity of the *Y* model, indicating that *Y* did not correlate with the *EDS′*. This fact also became obvious when comparing the experimental data of the *EDS* shown in Figure 2 with the *Y* data in Figure 1. The *EDS* decreased with increasing w_{TSA}, ϑ and t_c. With a w_{TSA} of 5%, the *EDS* decreased from 11 ± 1.5 by cross-linking at 120°C for 60 min to 1.8 ± 0.5 at 160°C for 90 min (Figure 2). By increasing w_{TSA} to 15%, low *EDS* values of 1.3 ± 0.1 were reached with the network PT-15-160-90-s. PT-10-140-75-s reached an *EDS* of 1.5 ± 0.10 With w_{TSA} of 15%, no higher *EDS* than 4.3 ± 1.0 (PT-15-120-60-s) were reached with the tested cross-linking parameters.

From a chemical perspective, it is conceivable that for *Y*, two competing processes are effective during thermal treatment of PVA with TSA. On the one hand, a cross-linking reaction takes place that increases *Y* and seems to be accelerated by higher ϑ and w_{TSA} and proceeds further by increasing t_c. The more chemical cross-links are formed, the higher is the fraction of insoluble material. This process is dominant at the milder cross-linking conditions (low ϑ, low t_c), in our example controlled by w_{TSA}. Moreover, an increasing number of cross-links results in the well-known reduction of *EDS* upon increase in cross-link density.[36,37]

On the other hand, a side reaction that is also accelerated by ϑ and especially with increasing w_{TSA} takes place that is obviously connected to a weight loss of the system, thus reducing the fraction of the starting material recovered after the experiments. This side reaction becomes dominant at the harsher reaction conditions (high ϑ, high t_c), but is also relevant for parameter combinations where only either ϑ or t_c is high, while the other value is low. As a result, in these cases *Y* decreases parallel to the *EDS*, indicating that the side reaction reduces hydrophilicity of the final polymer network.

In order to support the reasoning that a side reaction is responsible for the mass loss at high ϑ, thermogravimetric analysis was performed. Here, the mass loss was measured without any washing step in contrast to the previous experiments, so that a mass loss would be a strong indication of decomposition reactions. The corresponding data are shown in Figure 3. The decomposition temperature of neat PVA was measured at 284°C, which is the onset of the first decomposition stage. For the PVA networks PT-15_120_60 (cross-linked PVA with $w_{TSA} = 15\%$, $\vartheta = 120$ °C, $t_c = 60$ min, no washing/swelling steps), PT-10_120_60 and PT-5_120_60, the onset temperature ϑ_{d1} of thermal decomposition decreased to 152, 156, and 163°C, respectively, which is quite close to the high value of $\vartheta = 160$°C used in the cross-linking experiments above. We observed the second decomposition temperature ϑ_{d2} at 466, 424, 423, and 421°C for crude PVA and PT-5_120_60, PT-10_120_60 and PT-15_120_60 respectively. Therefore, ϑ_{d2} decreased in comparison to crude PVA.

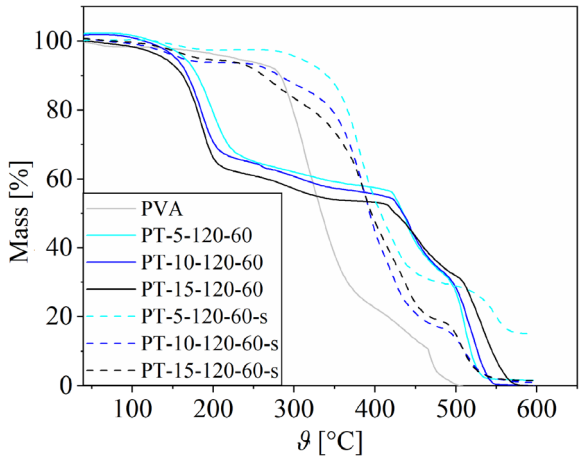

FIGURE 3 Thermogravimetric analysis of neat polyvinyl alcohol (PVA), PVA cross-linked for 1 h at 120°C in presence of *p*-toluenesulfonic acid (TSA) with (PT-5-120-60-s, PT-10-120-60-s, PT-15-120-60-s) and without (PT-5-120-60, PT-10-120-60, PT-15-120-60) washing with 50 mmol L^{-1} $NaOH_{(aq)}$ for 3 h at 90°C and water for 24 h at 90°C. Compared to pure PVA, the degradation temperature ϑ_{d1} decreased from 284 to 152°C for PVA networks containing 15% (w/w) TSA, 154°C for 10% (w/w) TSA and to 163°C for 5% (w/w) TSA. Neutralization of excess protons via washing of the specimens raised ϑ_{d1} to 325, 336 and 341°C, respectively [Color figure can be viewed at wileyonlinelibrary.com]

Generally, intact and insoluble polymer networks were fabricated by cross-linking PVA in presence of TSA. From our point of view, the optimal operation point regarding *Y* and *EDS* is 5% (w/w) TSA, at 120°C and 90 min cross-linking period. The gel content of $78\% \pm 2.0\%$ ensures intact hydrogels while the *EDS* of 4.6 ± 1.1 is high compared to other hydrogels presented in this paper, which indicates good hydrophilicity. However, it can be hypothesized that there might be issues concerning the long-term stability of the formed polymer networks. Both the side-reactions as well as the cross-linking reaction might proceed also at lower temperatures than used for cross-linking, changing the material properties over time. Therefore, in the next step, data helpful for the identification of the cross-linking as well as the side-reaction will be generated in order to be able to take measures for stabilization of the formed polymer network.

3.2 | Chemical reactions in the PVA/TSA mixture

As discussed above, it is likely that two competing reactions are effective when heating a mixture of PVA and TSA: One reaction that leads to cross-linking and one

reaction that leads to weight loss together with reduced hydrophilicity.

FT-IR spectroscopy was used to assess changes of the chemical composition induced by heating, also for longer time periods than used for the cross-linking investigations (Figure 4a and Figure 4b). A C=O stretching vibration of the not fully hydrolyzed ester functionalities was observed at 1684 cm^{-1} in neat PVA (Figure 4a). By heat treatment at 120°C in the presence of TSA, the most prominent change in the spectra are two new absorption bands at 1640 and 1710 cm^{-1}. They were assigned to C=O and C=C stretching vibrations. Their intensity was rather low directly after cross-linking, but in samples washed only with water after cross-linking, a longer thermal treatment of samples up to 24 h strongly increased their intensity (Figure 4a). Concomitantly, the band between 3000 and 3500 cm^{-1} connected to OH stretching vibrations decreased. Also at wavenumbers smaller than 1500 cm^{-1}, the spectra changed markedly. However, it was difficult to assign these changes to specific functional groups. Longer treatment times were also connected to a change of the sample appearance, that is, the samples

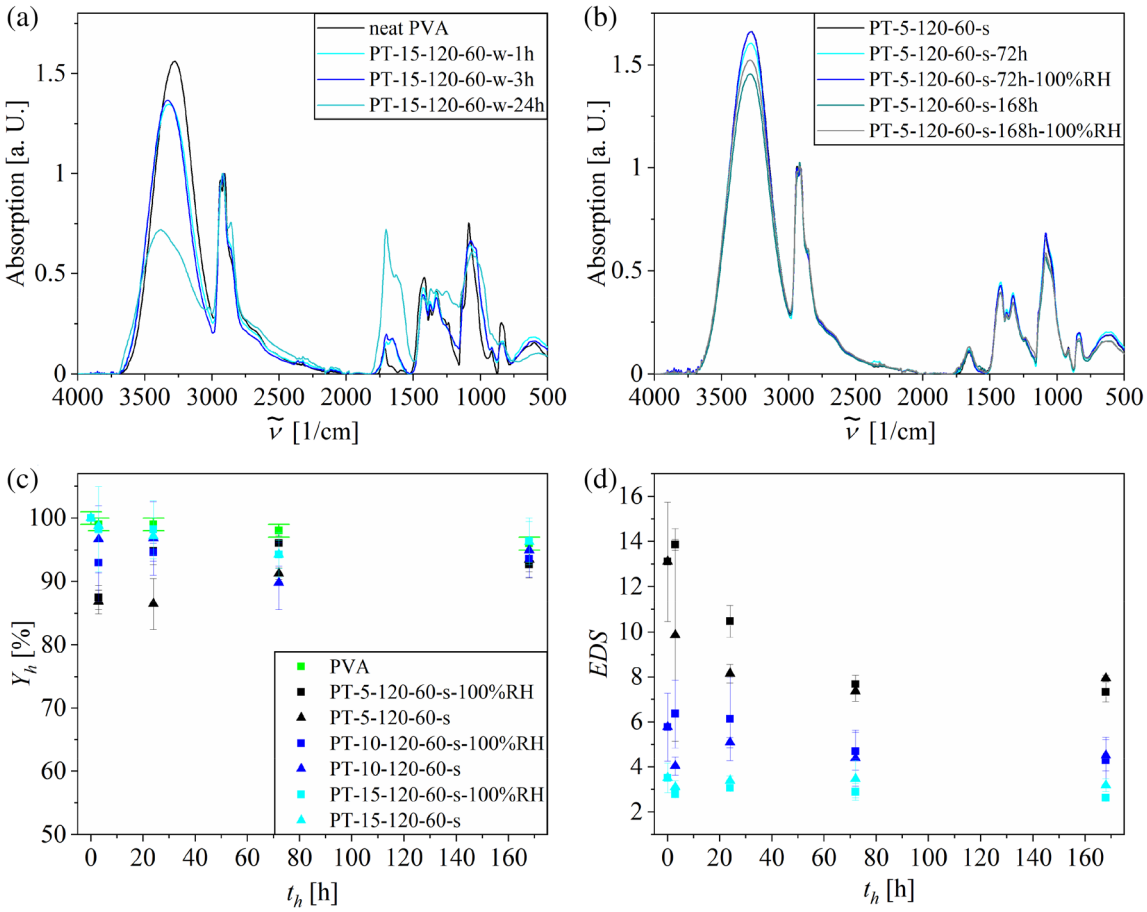

FIGURE 4 Investigation of the thermal stability of cross-linked polyvinyl alcohol (PVA)/*p*-toluenesulfonic acid (TSA) networks at 120°C. (a) Fourier transform infrared (FT-IR) spectra of water washed networks heat-treated with t_h = 1, 3, and 24 h, respectively. The crude PVA reference was not washed, because it would completely dissolve. PT-15-120-60-w networks showed increasing carbonyl and vinyl stretching vibrations at 1640 and 1710 cm^{-1}, respectively, indicating that chemical reactions took place during heat treatment. (b) FT-IR spectra of networks washed with the extended washing protocol, including a washing step with aqueous sodium hydroxide solution. Samples were heat-treated for 72 and 168 h in dry and water saturated air, respectively. Neutralization of the TSA after cross-linking (PT-15-120-60-s) inhibited changes in the FT-IR spectra. Heat treatment of PT-15-120-60-s in water saturated air (PT-15-120-60-s-100% RH) did not change the FT-IR spectra, either. Spectra of the networks PT-5-120-60-s and PT-10-120-60-s are given in figure S3 (supporting information). (c) Y_h and (d) *EDS* of the samples washed with the extended washing protocol (legend relevant for both datasets). No steady decrease of Y_h with increasing t_h was observed. The *EDS* of the network PT-5-120-60-s decreased between t_h of 3= and 72 h, indicating the formation of further cross-links. Only minor changes in Y_h, *EDS* and FT-IR spectra between t_h of 72 and 168 h were observed for all neutralized networks. Therefore we conclude, that a stable state regarding to the amount of cross-links and chemical properties was reached [Color figure can be viewed at wileyonlinelibrary.com]

became increasingly brown as shown in Figure S2 (supporting information). Taken together, we conclude that chemical reactions take place also after the designated cross-linking period, meaning that the samples properties are not stable over longer times.

We ascribed the assignable changes in the FT-IR spectra mainly to decomposition reactions of the PVA by elimination and oxidation reactions. The formation of C=C and C=O groups due to heat treatment of PVA was observed before by Matsubara and Imoto.[38] Tsuchiya et al.[39] found aldehydes, methyl ketones and water as the main thermal decomposition products of PVA. Both studies fit our observations and support that thermal degradation is taking place. These degradation reactions were obviously accelerated by TSA, as visible in the TGA data in Figure 3. This also is in line with the increasing mass loss as t_c and w_{TSA} were increased at high ϑ (Figure 1), as well as with the reduced hydrophilicity (Figure 2). Another side reaction in the PVA/TSA system might be the formation of sulfonic esters, as described in Section 1, for example, for the PVA/PSSA system. Sulfonic ester bands[29] were expected around 1460 and 1170 cm^{-1}. However, no bands at these wavenumbers could clearly be assigned to a sulfonic ester group in our spectra. Concerning the cross-linking reactions, no clear conclusions could be drawn from the FT-IR spectra. As described in Section 1, TSA might catalyze the formation of ether bonds involving two PVA hydroxyl groups. The corresponding C—O—C stretching vibration would be expected to occur between 1150 and 1070 cm^{-1}, but is not clearly visible. The only indirect indication is given by the reduction of the OH stretching vibration, as two hydroxyl groups are consumed per ether bond cross-link, but this cannot clearly be distinguished from elimination reactions.

In order to clarify whether cross-linking is likely to proceed via ether bond formation and to find out if sulfonic ester bonds are formed under the reaction conditions, we carried out a model reaction using 2-propanol as a PVA substitute, resulting in soluble products that can easily be analyzed by ^{1}H NMR spectroscopy. The reaction conditions and outcomes are listed in Table S2 (Supporting Information), the corresponding ^{1}H NMR spectra in Figure S1. Generally, at all reaction conditions, distinct formation of diisopropylether was observed, whereas the sulfonic ester isopropyltosylate was observed only in trace amounts. The conversion χ of 2-propanol to diisopropylether was increased both by increasing the reaction time as well as by adding silica gel as a drying agent, the latter indicating that water participates in a dynamic equilibrium reaction like acid-catalyzed ether bond formation. The highest χ of 0.14 was found after 3 h reaction time with 0.1 eq. TSA with silica gel. This means that under these conditions, 1.2 ether bonds per TSA molecule were formed, also in line with TSA rather being a catalyst than a reactant.

From the model experiment, we tend to conclude that cross-linking of PVA with TSA proceeds via ether bond formation, and that formation of sulfonic esters is only of minor importance. However, experiments by Chandra et al.[26] showed that sulfonic ester formation depends on the solvent. They observed the formation of sulfonic esters by the reaction of TSA with butanol in toluene, but had no yield in water, DMF and *o*-xylene. Therefore, it cannot be completely ruled out that the reaction outcome in PVA matrix might differ from the reaction in 2-propanol.

Summarizing, the interplay of cross-linking via ether bond formation on the one hand and thermal degradation via elimination of water and oxidation on the other hand is likely to cause the experimental findings on *Y* and *EDS* (Figures 1 and 2), similar to what was described by Immelman[21] for the PVA/sulfuric acid system. Thermal degradation is favored over cross-linking at higher temperatures in the PVA/TSA system. This is in agreement with the general observation, that elimination is favored over ether bond formation via nucleophilic substitution when increasing the temperature and Brønsted acid concentration.[22] The data makes it safe to conclude that cross-linking indeed occurs at all and that the formation of insoluble material is not solely caused by hydrophobization after elimination of water. These findings are also relevant when looking at other literature reports for treatment of PVA with acidic compounds, for example, by Xu et al. who treated sulfated PVA thermally.[24] Their acidic sulfonic acid groups could have catalyzed the ether bond formation between two hydroxyl groups of two different polymer chains, which could have led to insolubility. The same cross-linking behavior could be the reason for the observations of Saito et al.[28] Their observed decreasing degrees of hydration while heat treatment of PVA in presence of PSSA may occur due to chemical cross-linking of the PVA via ether bonds. However, the presence of an acidic compound at temperatures of 140–180°C can lead to the elimination of the hydroxyl groups in PVA and will therefore decrease the *EDS* and the solubility in water, too. The formation of ether bonds and the elimination of hydroxyl groups might occur at the same time at temperatures of 120–160°C, when a sulfonic acid is present.

From the FT-IR spectra (Figure 4a), it was concluded that washing with water is not enough to avoid side reactions and further thermal decomposition at relatively low temperatures. It can be expected that the same is true for the cross-linking reaction. However, chemical reactions that change the composition and therefore the properties of the PVA network are problematic for any application.

Therefore, we aimed to identify a suitable method to increase the thermal stability of the polymer networks. We hypothesized that washing with water alone is not sufficient to remove TSA completely from the samples, so that remaining acid keeps catalyzing chemical reactions.

Therefore, the samples were washed with aqueous solutions of sodium hydroxide after cross-linking, followed by water. The obtained samples were then heated to assess their thermal stability over time and studied by TGA (Figure 3) and FT-IR spectroscopy (Figure 4b) similar to the samples described above that were only washed with water. After this extended washing method, the PVA networks showed no visible increase of the C═C and C═O stretching upon further thermal treatment. This indicated that in fact the thermal decomposition was effectively avoided. Also the TGA measurements showed increased ϑ_{d1} around 330°C and increased ϑ_{d2} around 500°C. This raise in decomposition temperatures was ascribed to the neutralization of the acid, rendering it ineffective as a catalyst. The decomposition temperatures of the neutralized polymer networks were higher than of PVA, which could be explained by the formation of ether cross-links. Sonker et al.[40] observed an increase in decomposition temperature due to aliphatic cross-linking of PVA with suberic acid. Another explanation is the partial dehydration while cross-linking. This effect was shown by Yang et al.[41] for thermally treated PVA without the presence of an acid.

In order to assess the effect of the extended washing protocol on the stability of the material properties during thermal treatment at 120°C, the cross-linked samples were observed for 1 week by measuring the heat treatment gel content Y_h and *EDS* (Figure 4c,d) in addition to the FT-IR spectra (Figure 4b). After the stability test, the samples were washed again at 90°C for 12 h in water to remove polymer chains, which were cleaved off the network. By dividing the mass of the networks before and after the stability test, the mass quotient Y_h was calculated (Equation 4). The neat PVA reference was not washed because it would completely dissolve. It showed a Y_h of 96% ± 1% after a heat treatment period t_h of 168 h in dry air (Figure 4c). The mass loss of 4% can be attributed to a loss of adsorbed water. All networks show high Y_h between 93% and 96% after a t_h of 168 h, which is approximately equal to the Y_h of neat PVA. Furthermore, no steady decrease in Y_h with increasing t_h was observed. Both indicates that no decomposition occurred. The *EDS* of the network PT-5-120-60-s and the same network heat-treated under humidified air (PT-5-120-60-s-100%RH) decreased from 9.9 ± 4.7 to 7.9 ± 0.1 and from 13.9 ± 0.2 to 7.3 ± 0.4, respectively (Figure 4d). The decreased *EDS* was not the result of decomposition, since no formation of C═C and C═O bonds were observed in the FT-IR spectra (Figure 4b). We hypothesized that the decreasing *EDS* was the consequence of a post-cross-linking, which led to decreased free volume and hydrophilicity of the networks. This effect can be illustrated by the decrease in *EDS* of the network PT-5-120-60-s between t_h of 3 and 72 h, while the mass loss stayed approximately constant. The decreasing *EDS* rather indicates a progressing cross-linking process than decomposition, since the latter would strongly decrease the overall mass of the networks (Figure 1) and Y_h. However, ether bond formation was unlikely, since the essential TSA had been deactivated by the extended washing protocol. The post-cross-linking is rather explained by the formation of physical cross-links. Wang et al.[42] showed that heat treatment of cross-linked PVA membranes at 120°C led to a decrease of the *EDS*. This effect was attributed to the crystallization of the membrane polymer. We propose, that the decreasing *EDS* with increasing t_h is caused by crystallization of our networks in the same way. PT-5-120-60-s showed lower *EDS* after t_h of 3 and 24 h compared to the analogous networks heat-treated in water saturated air (PT-5-120-60-s-100% RH). The same correlation between the *EDS* values was observed when comparing the PT-10-120-60-s networks, yet the difference is smaller and diminishes completely when comparing the PT-15-120-60-s networks. However, the difference in *EDS* between heat treatment in dry and humidified air indicates a slower post-cross-linking while heat treatment in humidified air compared to dry air. This is in good agreement with the crystallization of the networks. We propose, that the humidified air led to absorption of water into the network, which slowed down the implementation of crystallinity. The lower the *EDS*, the smaller the effect, since less water can be absorbed by the hydrogel networks. Thus, the difference in *EDS* was highest at the PT-5-120-60-s networks, when comparing heat-treatment in dry and humidified air.

PT-5-120-60-s reached the minimum *EDS* possible for this specific parameter set after 72 h. Increasing t_h to 168 h showed no further difference in *EDS*. In contrast, a stable *EDS* was reached by PT-15–120-60-s already directly after cross-linking ($t_h = 0$ h) and was with 3.1 ± 0.3 the lowest observed value. Extending t_h had no influence on the *EDS* or the mass. These observations indicate that there was no further post-cross-linking while heat treatment after 72 h for the network PT-5-120-60-s and none at all for the network PT-15–120-60-s. This is in good agreement to the influence of polymer crystallization on the *EDS*. According to our conclusions, the most PVA hydroxyl groups were consumed for the formation of ether bonds, elimination and oxidation when heat cross-linking with the highest amount of TSA present. Hence, the PT-15-120-60-s

networks had the lowest *EDS* before the stability test ($t_h = 0$, Figure 4d). Crystallization of those networks had only a minor influence on the *EDS*, since it was already low. Moreover, the small relative amount of hydroxyl groups is disadvantageous for the crystallization of PVA. However, the differences in *EDS* and Y_h between t_h of 72 and 168 h were within the standard deviation for all observed networks. Therefore, we conclude that it is possible to reach a stable state concerning decomposition, cross-linking and hydrolysis for PVA networks cross-linked with TSA at operating temperatures up to 120°C and varying relative humidity within a t_h of 168 h.

Considering the decreased ϑ_{d1} of PVA in presence of TSA in the TGA experiments, the behavior of C=C and C=O vibrations in the measured FT-IR spectra, the stability experiments in dry and humidified air, the published results on the thermal decomposition of PVA[38,39,41] and the observed reactions of PVA in presence of sulfuric acid,[21,23] we propose that the decomposition of PVA in presence of TSA occurs via dehydration and oxidation at lowered temperatures and increased rate compared to crude PVA. Neutralization of TSA in the PVA networks by washing with aqueous NaOH solution and water removes the negative effect on the thermal stability. In addition, we conclude that due to cross-linking and slight dehydration the PVA networks show increased decomposition temperatures in comparison to neat PVA in TGA experiments, which resulted in sufficient temperature stability for the observed time periods.

3.3 | Cross-linked polyvinyl alcohol coatings on polyvinylidene fluoride hollow fibers for water vapor transport

In order to demonstrate the potential of the PVA/TSA cross-linking system for applications, PVA/TSA coatings were prepared on PVDF HF, cross-linked by thermal treatment and washed with the extended washing protocol described above. Details on the PVDF HFs are described in a previous study by Jesswein et al.[9] The resulting composite membranes were then tested for their water vapor transfer rates (*WTR*). Cross-linker concentration $w_{TSA} = 10\%$ was chosen, since the evaluation of the cross-linking experiments of the pure networks showed a faster cross-linking velocity compared to $w_{TSA} = 5\%$ and higher *EDS* compared to $w_{TSA} = 15\%$ networks (Figures 1 and 2). Therefore, the networks with $w_{TSA} = 10\%$ are a good compromise between high Y at minimized cross-linking periods, good hydrophilicity and minor formation of physical cross-links due to post-cross-linking, which is beneficial for the water vapor transfer, and improved thermal stability compared to crude PVA. The layers were cross-linked at the lowest possible ϑ (120°C) in order to minimize the thermal stress on the PVDF HF membrane carrier and the decomposition of the PVA layer. t_c was varied between 60 and 180 min towards optimization of the membrane performance by changing the *EDS* and Y of the layers. However, we expect that the heat distribution while cross-linking differs between thin layers on HF and thicker free standing PVA samples, which could have an influence on the cross-linking velocity. Therefore, scanning electron microscopy (SEM) images were recorded after processing the cross-linked membranes with the extended washing protocol, in order to verify that an intact and insoluble PVA layer adhered on the HF.

Cross-section SEM images showed dense PVA layers on the surface of the PVDF fibers (Figure 5). There was no impregnation of the fibers. Furthermore, homogeneous layers were reached for all cross-linking periods, for example, 60 min (Figure 5a) and 120 min (Figure 5b). The determined average thickness of the PVA layer via SEM was 2.8 ± 0.6 μm. SEM pictures and layer thickness are comparable to pure PVA coatings on PVDF fibers which where cross-linked with glutaraldehyde in a second step.[9] Therefore, we conclude that the TSA content in the coating solution had no or a negligible influence on the layer homogeneity and thickness.

According to the solution-diffusion model, the permeation of gases decreases with increasing thickness of the selective layer.[43] Since we want to use the PVA layer to achieve a good selectivity of water against air while maintaining a high water vapor permeance, a thin layer was preferred. However, thin selective layers may reduce the selectivity since inhomogeneity and defects more likely introduce leakages into the membrane. Possible leakages in the membrane will strongly increase the nitrogen permeance. Therefore, the nitrogen permeance is an important parameter to verify the success of the membrane fabrication process. The nitrogen permeance J_N of the membranes was measured after cross-linking and neutralization according to the extended washing protocol. J_N values of composite PVA/PVDF HF membranes with varying t_c before and after the water transfer measurement (WTR-M) are shown in Figure 6.

J_N decreased by three orders of magnitude, comparing the uncoated reference HF with the composite PVA/PVDF HF membranes. In good agreement with the observed layers on the PVA/PVDF HF composite membranes in SEM (Figure 5), we conclude that the cross-linked PVA coatings are dense and homogeneous over the complete fiber length. The coating and cross-linking process was successful. However, swelling of the PVA layers while measuring the *WTR* could introduce defects and delaminate the membrane. Both would lead to an

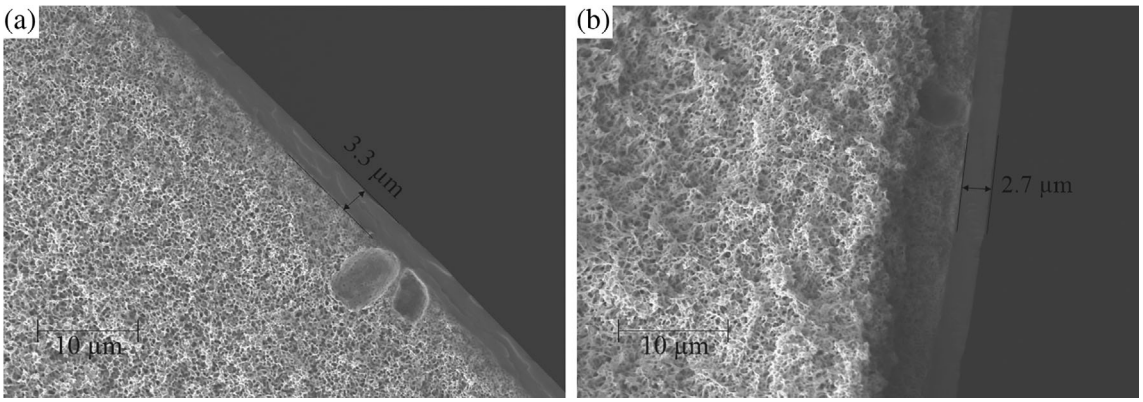

FIGURE 5 Cross-section scanning electron microscopy images of polyvinyliden fluoride (PVDF)/polyvinyl alcohol (PVA) hollow fiber membranes. (a) $t_c = 1$ h. (b) $t_c = 2$ h. The fibers were washed with NaOH (aq) and water as described above for the PVA networks before the images were taken. All images show dense PVA layers with an average thickness of 2.8 ± 0.6 µm and no impregnation of the PVDF hollow fibers

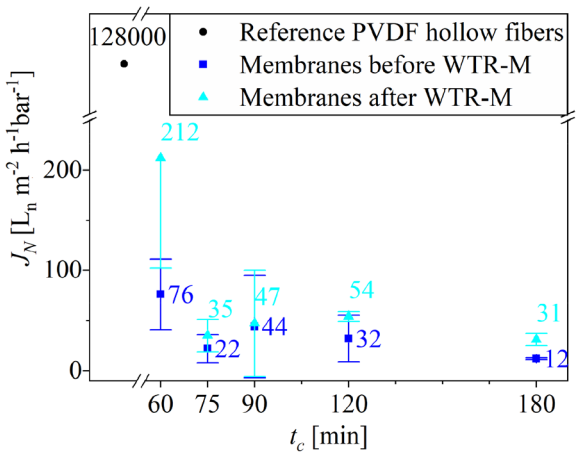

FIGURE 6 Nitrogen permeance J_N of polyvinyliden fluoride (PVDF)/polyvinyl alcohol (PVA) hollow fiber (HF) composite membranes cross-linked for 1, 1.5, 2, and 3 h before and after the water transfer measurement (WTR-M). As a reference, the average J_N of nine uncoated PVDF hollow fiber membranes was included in the plot. All PVA/PVDF composite membranes showed a decrease in J_N by 3 orders of magnitude compared to the reference PVDF HF fibers, indicating a dense PVA coating before and after the WTR-M [Color figure can be viewed at wileyonlinelibrary.com]

increase of J_N. However, an analysis of variance showed that the WTR-M had no significant influence on J_N. Moreover, the measured differences in J_N before and after WTR-M, are minor compared to the J_N decrease caused by the PVA coating onto the HF. Therefore, we conclude, that no significant leakages were introduced into the membrane while measuring the *WTR*. The fabricated composite PVA/PVDF HF membranes stayed intact. One should note that t_c was significant with a p-value of 0.008, indicating that longer t_c decreased J_N. The Bonferroni test narrowed the result down to significant differences between membranes cross-linked with $t_c = 60$ min and membranes with longer t_c. The reason behind this was the complex correlation between t_c and Y (Figure 1). In the case of cross-linking with $t_c = 60$ min, $w_{TSA} = 10\%$ and $\vartheta = 120°C$, longer cross-linking resulted in increased Y. Higher Y resulted in lower J_N, since the cross-link density of the layer was possibly higher and therefore less permeable.

The absolute J_N of the composite PVA/PVDF HF membranes were between 4.44 ± 0.0370 GPU before the WTR-M and 78.5 ± 40.7 GPU after the WTR-M. Liu et al.[44] achieved selective layers of poly(dopamine) modified PVA on PVDF HF with a thickness of 450 nm and J_N between 1500 and 2500 GPU. Our observed J_N values were more than one magnitude lower, which can be explained by the higher PVA layer thickness. PVDF HF composite membranes with glutaraldehyde cross-linked PVA coatings showed J_N of approximately 60 L m^{-2} h^{-1} bar^{-1},[9] that is comparable to our observed values. Thus, heat cross-linking of PVA in presence of TSA did not lead to high J_N compared to other PVA coatings used for water vapor transport.

In summary, the PVA/PVDF HF composite membranes presented in this paper showed approximately three magnitudes lower J_N after the extended washing protocol and the WTR-M, compared to the uncoated PVDF HF membranes. The absolute J_N values were comparable to other PVA composite membranes. Therefore, we conclude that PVA layers cross-linked at 120°C in presence of TSA show good barrier properties against nitrogen at all t_c and they are stable in liquid water and humidified air at temperatures up to 90°C. The humidification performance of the PVA/PVDF HF composite membranes was analyzed by measuring the water transfer rates (*WTR*).

The highest *WTR* were measured for the membranes with $t_c = 60$ min, for example, 3.24 ± 0.040 kg m^{-2} h^{-1} compared to 3.04 ± 0.030 kg m^{-2} h^{-1} with $t_c = 180$ min at 80°C and 100 mL$_n$ min^{-1} (Figure 7). This correlation can be explained with the *EDS* of the cross-linked PVA layers. The *EDS* of the networks with $t_c = 60$ min (e.g., PT-5-120-60-s) were the highest observed values in Figure 2. Therefore, the highest degree of hydrophilicity and mesh size was expected for the selective PVA membrane layers consisting of these networks. Both is beneficial for the water vapor permeance. Moreover, it was expected that the networks with the highest *EDS* show the strongest plasticization effect. Plasticization is often accompanied by an increased free volume and a lowered glass transition temperature T_g due to an increased chain mobility at sorbent partial pressures close to saturation. A higher permeant diffusion coefficient in the membrane can be its consequence.[43,45] This is in good agreement with our observed *WTR* values, as they are highest for membranes with $t_c = 60$ min, where we expect the highest plasticization.

The overall *WTR*s increased with increasing measurement temperature ϑ_P, that is, membranes cross-linked with a t_c of 180 min showed *WTR*s of 0.83 ± 0.01, 1.52 ± 0.02, 3.04 ± 0.03 and 5.61 ± 0.10 kg m^{-2} h^{-1} at air volume flows $\dot{V}_n$ of 100 mL$_n$ min^{-1} and ϑ_P of 60, 70, 80, and 90°C, respectively. The increase in *WTR* can be attributed to a higher water vapor partial pressure and stronger swelling of the membrane layers. Furthermore, the diffusion coefficient of water in the membrane increases with ϑ_P, which could lead to an increased *WTR*. This behavior is typical for a diffusivity driven water vapor transport mechanism as described, for example, for Teflon membranes.[46] Composite PVA/PVDF HF membranes showed increasing *WTR*s with increasing $\dot{V}_n$. The steady increase was observed for all membranes at ϑ_P up to 80°C. This was expected, because the water vapor partial pressure gradient is the driving force for the water transfer. $\dot{V}_n$ influences this gradient through variation of the water vapor partial pressure at the feed side, as well as the flow conditions. Furthermore, increasing water vapor partial pressure leads to stronger swelling. Analogous dependence of water transfer through membranes and water activity is widely observed.[8,13,47] The measurements at $\vartheta_P = 90$°C were in contradiction to this correlation. Furthermore, the data showed a higher slope of the *WTR* increase at lower $\dot{V}_n$ for all ϑ, but especially at 90°C, where the slope turned negative at $\dot{V}_n = 125$ mL$_n$ min^{-1}. The reason behind this trend inversion were limitations of the measuring method. At high ϑ_P and $\dot{V}_n$ it was not possible to hold the water vapor partial pressure at the feed side on a constant value, for example, it decreased at $\vartheta_P = 90$°C from 0.68 bar at 25 mL$_n$ min^{-1} to 0.63 bar at 200 mL$_n$ min^{-1}. With decreasing water vapor partial pressure on the feed side, the concentration gradient decreases which lowers the *WTR*.

At $\vartheta_P = 80$°C and $\dot{V}_n = 200$ ml$_n$ min^{-1}, a *WTR* of 3.89 ± 0.09 kg m^{-2} h^{-1} was reached with $t_c = 60$ min, whereas the 90 min cross-linked membrane showed a *WTR* of 3.15 ± 0.03 kg m^{-2} h^{-1}. The increase in *WTR* of 23% due to the shorter cross-linking period, decreased to a 17% increase when lowering ϑ_P to 70°C. At $\vartheta_P = 90$°C, the *WTR* difference between the membranes cross-linked with $t_c = 60$ min and $t_c = 90$ min was at a maximum of 26%. One could explain this observation with the temperature dependence of the *EDS*. The absolute differences of the *EDS* between membrane layers with varying t_c increases with ϑ_P. At $\vartheta_P = 90$°C the highest possible *EDS* differences due to varying t_c showed the highest differences in the *WTR*s, consequently. The same correlations were observed with increasing $\dot{V}_n$ instead of ϑ_P.

The *WTR*s at $\vartheta_P = 80$°C were converted to the permeance J_W in GPU (Equation 8 and section 5 in supporting information). Moreover, the ratio of water and nitrogen permeance Q_{WN} (Equation 9) was calculated. The highest J_w and Q_{WN} values of membranes produced with $t_c = 180$ min at $\vartheta_P = 80$°C were 6423 GPU $\pm$ 63.0 GPU and 1445 ± 114, respectively. These values were reached at $\dot{V}_n = 100$ ml$_n$ min^{-1}. One should note that J_N was measured at room temperature with dry nitrogen and J_w at 80°C in wet air, which has an impact on Q_{WN}.

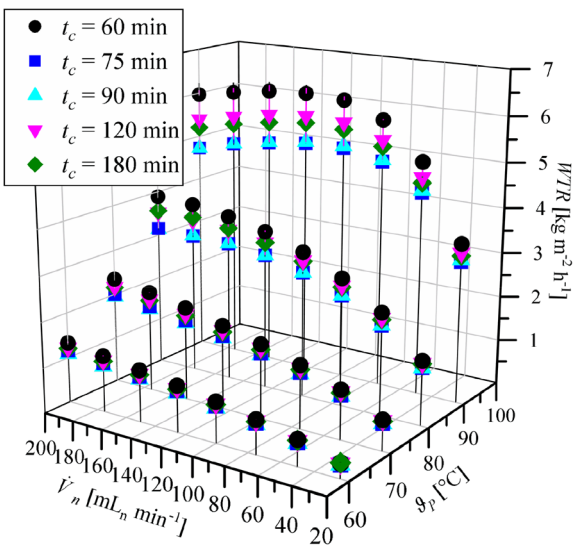

FIGURE 7 Water transfer rates (*WTR*) of composite polyvinyliden fluoride/polyvinyl alcohol hollow fiber membranes cross-linked in the presence of TSA at 120°C with a t_c of 60, 75, 90, 120, and 180 min, respectively. The *WTR*s were measured at varying ϑ_P between 60 and 90°C and volumes flows $\dot{V}_n$ between 25 and 200 ml$_n$ min^{-1}, respectively [Color figure can be viewed at wileyonlinelibrary.com]

Liu et al.[35] reached a J_w of 2298 GPU with a zeolite filled PVA/PVDF membrane at a ϑ_P of 25°C. This value is more than 50% lower than our measured values. However, the water vapor permeance is strongly dependent on ϑ_P, which was 80°C in our measurement. Liu et al.[44] moreover reported that PVA/PVDF hollow fiber membranes surface modified with poly(dopamine) reached a J_w of 2898 GPU and a selectivity against nitrogen S_{WN} of 2.09 at $\vartheta_P = 25$°C. The determined Q_{WN} of our TSA cross-linked membranes was 1445 at $\vartheta_P = 80$°C, which represents a difference of three magnitudes. The main reason for this difference were the lower J_N values of the TSA cross-linked composite PVA/PVDF HF membranes. Tong et al.[48] fabricated Lupamin© membranes on a polysulfon support with J_w between 2250 and 4000 GPU at $\vartheta_P = 120$°C. The measured water vapor permeances are therefore in the same dimension as the J_W of the presented composite PVA/PVDF HF membranes in this work. In summary, the here presented membranes show comparable J_w and Q_{WN} to other water vapor permeable membranes. Therefore, we conclude that PVA cross-linked in presence of TSA is an interesting semipermeable layer for composite membranes in water vapor separation systems, that is, humidifier membranes.

4 | CONCLUSIONS

Our study contributed to a further understanding of the cross-linking and thermal degradation of PVA in the presence of TSA. It was proven, that TSA can be used to cross-link PVA. A potential application for PVA cross-linked with TSA as selective layer on a PVDF HF humidification membrane has been shown. For this purpose, PVA was cross-linked with TSA at different values of ϑ, w_{TSA} and t_c. Y increased with increasing ϑ and t_c with $w_{TSA} = 5\%$. With $w_{TSA} = 15\%$ the trend turned vice versa. This behavior was attributed to the coexistence of a cross-linking reaction and thermal decomposition. The latter became dominant with increasing ϑ and t_c. The cross-linked networks showed inferior ϑ_d in comparison to crude PVA. The presence of TSA in the PVA networks led to formation of carbonyl and vinyl groups in the network when heating them to 120°C. Neutralization of the excess acid and washing of the networks recovered the thermal stability and even improved it to higher ϑ_d compared to crude PVA. Moreover, oxidation and elimination were suppressed. After 72 h heat treatment in dry or humidified air, a stable state regarding *EDS* and Y_h was reached. Through an experiment with 2-propanol as model substance, the formation of ether bonds was identified as predominant for cross-linking PVA in presence of TSA. Therefore, we conclude that nucleophilic substitution, elimination and oxidation are the predominant reactions while heat treatment of PVA in presence of TSA, analogous to sulfuric acid. Composite PVA/PVDF HF membranes were fabricated by coating PVDF HF with PVA and heat cross-linking in presence of TSA. The PVA layers were dense and no impregnation was observed. At $\vartheta_P = 80$ °C a J_w of 6423 GPU ± 63.0 GPU and a Q_{WN} of 1445 ± 114 was reached. In summary, heat cross-linked PVA in presence of TSA can be used as thermal degradation stable and easy to produce selective layer for humidifier membranes, that is, on PVDF HF support.

ACKNOWLEDGMENTS

This work was supported by the *Bundesministerium für Wirtschaft und Energie* (Germany) in the project *Hochintegriertes Kathodensubsystem* (grant ID 03ET6091D). We gratefully thank Monika Riedl for the SEM measurements and Marita Southan for preliminary membrane preparation experiments. Open access funding enabled and organized by Projekt DEAL.

CONFLICT OF INTEREST

The authors declare no conflict of interest.

ORCID

Günter E. M. Tovar https://orcid.org/0000-0002-2437-3405
Thomas Schiestel https://orcid.org/0000-0002-5214-7237
Alexander Southan https://orcid.org/0000-0001-7530-1690

REFERENCES

[1] Y. Shao, Y. Wang, S. Q. Cao, Y. J. Huang, L. F. Zhang, F. Zhang, C. R. Liao, Y. P. Wang, *Sensors* **2018**, *18*, 2029.
[2] C. F. Mok, Y. C. Ching, F. Muhamad, N. A. Abu Osman, N. D. Hai, C. R. C. Hassan, *J. Polym. Environ.* **2020**, *28*, 775.
[3] R. Rodríguez-Rodríguez, H. Espinosa-Andrews, C. Velasquillo-Martínez, Z. Y. García-Carvajal, *Int. J. Polym. Mater. Polym. Biomater.* **2020**, *69*, 1.
[4] S. Miar, C. A. Perez, J. L. Ong, T. Guda, *J. Biomater. Appl.* **2019**, *34*, 523.
[5] R. H. Li, T. A. Barbari, *J. Membr. Sci.* **1995**, *105*, 71.
[6] F. B. Peng, X. F. Huang, A. Jawor, E. M. V. Hoek, *J. Membr. Sci.* **2010**, *353*, 169.
[7] A. Saraf, K. Johnson, M. L. Lind, *Desalination* **2014**, *333*, 1.
[8] S. D. Bhat, A. Manokaran, A. K. Sahu, S. Pitchumani, P. Sridhar, A. K. Shukla, *J. Appl. Polym. Sci.* **2009**, *113*, 2605.
[9] I. Jesswein, T. Hirth, T. Schiestel, *J. Membr. Sci.* **2017**, *541*, 281.
[10] Y. T. Hu, K. Lu, F. Yan, Y. L. Shi, P. P. Yu, S. C. Yu, S. H. Li, C. J. Gao, *J. Membr. Sci.* **2016**, *501*, 209.
[11] M. J. Park, R. R. Gonzales, A. Abdel-Wahab, S. Phuntsho, H. K. Shon, *Desalination* **2018**, *426*, 50.
[12] J. B. Gilbert, J. J. Kipling, B. McEnaney, J. N. Sherwood, *Polymer* **1962**, *3*, 1.

[13] S. J. Metz, W. J. C. van de Ven, J. Potreck, M. H. V. Mulder, M. Wessling, *J. Membr. Sci.* **2005**, *251*, 29.
[14] B. Bolto, T. Tran, M. Hoang, Z. L. Xie, *Prog. Polym. Sci.* **2009**, *34*, 969.
[15] A. S. Hickey, N. A. Peppas, *J. Membr. Sci.* **1995**, *107*, 229.
[16] M. G. Katz, T. Wydeven, *J. Appl. Polym. Sci.* **1982**, *27*, 79.
[17] M. Nagura, N. Takagi, T. Koyano, Y. Ohkoshi, N. Minoura, *Polym. J.* **1994**, *26*, 675.
[18] R. S. Harland, N. A. Peppas, *Colloid Polym. Sci.* **1989**, *267*, 218.
[19] K. C. S. Figueiredo, T. L. M. Alves, C. P. Borges, *J. Appl. Polym. Sci.* **2009**, *111*, 3074.
[20] C. K. Yeom, K. H. Lee, *J. Membr. Sci.* **1996**, *109*, 257.
[21] E. Immelman, R. D. Sanderson, E. P. Jacobs, A. J. Vanreenen, *J. Appl. Polym. Sci.* **1993**, *50*, 1013.
[22] P. Y. Bruice, *Organic Chemistry*, Pearson/Prentice Hall, Upper Saddle River, NJ **2011**.
[23] L. Drechsel, P. Görlich, *Infrared Phys.* **1963**, *3*, 229.
[24] J. M. Xu, H. Z. Ni, S. Wang, Z. Wang, H. X. Zhang, *J. Membr. Sci.* **2015**, *492*, 505.
[25] R. R. Choudhury, J. M. Gohil, S. Mohanty, S. K. Nayak, *Int. J. Polym. Anal. Charact.* **2019**, *24*, 334.
[26] J. Chandra, R. Chaudhuri, S. R. Manne, S. Mondal, B. Mandal, *ChemistrySelect* **2017**, *2*, 8471.
[27] A. Teasdale, E. J. Delaney, S. C. Eyley, K. Jacq, K. Taylor-Worth, A. Lipczynski, W. Hoffmann, V. Reif, D. P. Elder, K. L. Facchine, S. Golec, R. S. Oestrich, P. Sandra, F. David, *Org. Process Res. Dev.* **2010**, *14*, 999.
[28] K. Saito, A. Tanioka, K. Miyasaka, *Polymer* **1994**, *35*, 5098.
[29] K. Koyama, M. Okada, M. Nishimura, *J. Appl. Polym. Sci.* **1982**, *27*, 2783.
[30] K. E. Gutowski, D. A. Dixon, *J. Phys. Chem. A* **2006**, *110*, 12044.
[31] D. C. French, D. S. Crumrine, *J. Org. Chem.* **1990**, *55*, 5494.
[32] M. D. Gernon, M. Wu, T. Buszta, P. Janney, *Green Chem.* **1999**, *1*, 127.
[33] F. Barr-David, B. F. Dodge, *J. Chem. Eng. Data* **1959**, *4*, 107.
[34] G. S. Parks, B. Barton, *J. Am. Chem. Soc.* **1928**, *50*, 24.
[35] Y. L. Liu, J. C. Su, X. Cui, S. C. Zhang, X. Z. Meng, L. W. Jin, *IOP Conf. Ser.: Earth Environ. Sci.* **2020**, *463*, 012096.
[36] P. J. Flory, J. Rehner, *J. Chem. Phys.* **1943**, *11*, 521.
[37] S. K. Manu, T. L. Varghese, S. Mathew, K. N. Ninan, *J. Appl. Polym. Sci.* **2009**, *114*, 3360.
[38] T. Matsubara, T. Imoto, *Makromol. Chem.* **1968**, *117*, 215.
[39] Y. Tsuchiya, K. Sumi, *J. Polym. Sci., A-1: Polym. Chem.* **1969**, *7*, 3151.
[40] A. K. Sonker, K. Rathore, R. K. Nagarale, V. Verma, *J. Polym. Environ.* **2018**, *26*, 1782.
[41] H. G. Yang, S. B. Xu, L. Jiang, Y. Dan, *J. Macromol. Sci., B: Phys.* **2012**, *51*, 464.
[42] Y. L. Wang, H. Yang, Z. L. Xu, *J. Appl. Polym. Sci.* **2008**, *107*, 1423.
[43] J. G. Wijmans, R. W. Baker, *J. Membr. Sci.* **1995**, *107*, 1.
[44] Y. L. Liu, Y. Y. Wei, J. C. Su, L. Y. Zhang, X. Cui, L. W. Jin, *J. Mater. Sci.* **2020**, *55*, 5415.
[45] Y. Yampolskii, I. Pinnau, B. Freeman, *Materials Science of Membranes for Gas and Vapor Separation*, Wiley, West Sussex, UK **2006**.
[46] C. A. Scholes, S. Kanehashi, G. W. Stevens, S. E. Kentish, *Sep. Purif. Technol.* **2015**, *147*, 203.
[47] C. A. Scholes, J. Y. Jin, G. W. Stevens, S. E. Kentish, *J. Polym. Sci., B: Polym. Phys.* **2015**, *53*, 719.
[48] Z. Tong, V. K. Vakharia, M. Gasda, W. S. W. Ho, *React. Funct. Polym.* **2015**, *86*, 111.

SUPPORTING INFORMATION

Additional supporting information may be found in the online version of the article at the publisher's website.

How to cite this article: A. Michele, P. Paschkowski, C. Hänel, G. E. M. Tovar, T. Schiestel, A. Southan, *J. Appl. Polym. Sci.* **2022**, *139*(6), e51606. https://doi.org/10.1002/app.51606